

UDC 546.86'87'24'22

PHASE RELATIONS IN THE $\text{Sb}_2\text{Te}_2\text{S}$ - $\text{Bi}_2\text{Te}_2\text{S}$ SYSTEM AND CHARACTERIZATION OF $\text{Sb}_{2-x}\text{Bi}_x\text{Te}_2\text{S}$ SOLID SOLUTIONS**¹F.R. Aliyev, ¹E.N. Orujlu, ^{1,2}D.M. Babanly, ³A.L. Mustafayeva**¹*Azerbaijan State Oil and Industry University, French - Azerbaijani University,
AZ 1010, Azadlig ave. 20, Baku, Azerbaijan*²*Institute of Catalysis and Inorganic Chemistry of MSE Azerbaijan Republic,
AZ 1143, H. Javid ave. 113, Baku, Azerbaijan*³*Baku State University,
AZ 1148, Z. Xalilov str. 23, Baku, Azerbaijan*e-mail: fariz_ar@hotmail.com

Received 25.03.2023

Accepted 01.06.2023

Abstract: The phase equilibria of the $\text{Sb}_2\text{Te}_2\text{S}$ - $\text{Bi}_2\text{Te}_2\text{S}$ system was studied by powder X-ray diffraction (PXRD), differential thermal analysis (DTA), scanning electron microscope (SEM) and energy dispersive X-ray (EDX) microanalysis. It was shown that due to incongruent melting of the $\text{Sb}_2\text{Te}_2\text{S}$ compound the system is non-quasibinary, but it is stable below the solidus and characterized by the formation of a continuous series of solid solutions with a tetradymite-like hexagonal structure. The lattice parameters were determined from powder diffraction patterns. It was established that the crystal lattice parameters of solid solutions vary linearly with composition.

Keywords: phase diagram, solid solutions, tetradymite-like structure, topological insulators.

DOI: 10.32737/2221-8688-2023-2-132-139

Introduction

Van der Waals (VdW) materials based on bismuth and antimony chalcogenides have received great interest thanks to their thermoelectric properties [1-5]. Thermal conductivity of such alloys is reduced due to the effective scattering of phonons, which causes an increase in thermoelectric properties. Such materials include in sodium-ion batteries, solar panels, new-generation generators, and refrigerators [6-10]. Recently, tetradymite-like layered phases have been confirmed as 3D topological insulator (TI) [11-13] phases of quantum matter, thereby giving a boost of interest to the layered tetradymite mineral – $\text{Bi}_2\text{Te}_2\text{S}$ and its analogues, as well as solid solutions and doped phases based on them [14-18]. The last investigations demonstrated that these materials have wide potential applications in optoelectronics, spintronics, quantum computing etc. [19-24].

The $\text{Bi}_2\text{Te}_2\text{S}$ tetradymite mineral melts congruently at 898 K and crystallizes in rhombohedral space group $R\bar{3}m$ with the unit cell parameters $a = 4,2648 \text{ \AA}$ and $c = 29,5882 \text{ \AA}$ [25]. In its crystal structure, Te–Bi–S–Bi–Te atoms are covalently bonded to form five-layer slabs, alternating along the c axis so that there are three five-layer slabs per unit cell. Due to strong intra-stack cation–anion bonds and the electroneutrality of the stack as a whole, these five-layer slabs are stable structural elements and bonded with each other by the VdW bonds along the c axis.

Literary data on phase equilibria of the Sb_2Te_3 - Sb_2S_3 system [26] show that the $\text{Sb}_2\text{Te}_2\text{S}$ compound melts incongruently at 758 K and has a very narrow region of primary crystallization from about 66.5 to 69 mol.% Sb_2Te_3 . The results of [26] confirm that this phase has a tetradymite-like structure in

hexagonal form with parameters $a=4.1675\text{\AA}$ and $c=29.483\text{\AA}$.

An analysis of the structural features of tetradymite and other tetradymite-like compounds [14, 18, 27-30] shows that, in a five-layer package, the substitution of atoms by related atoms in both cationic and anionic positions is possible. Primary compounds of the system have close lattice parameters and the same space group. This allows them mix to the solid state and form a continuous series of solid

solutions below the solidus.

One of the important approaches to the development of new advanced materials is the study of phase diagrams composed of known compounds possessing desired functional properties [31, 32]. The $\text{Sb}_2\text{Te}_2\text{S}-\text{Bi}_2\text{Te}_2\text{S}$ system is interesting in terms of search for solid solutions with $\text{Bi} \leftrightarrow \text{Sb}$ substitution based on ternary compounds possessing tetradymite like layered structure.

Experimental part

High-purity (99.999%) elements from Alfa Aesar were used for the synthesis of the initial phases and the alloys of different compositions along the $\text{Sb}_2\text{Te}_2\text{S}-\text{Bi}_2\text{Te}_2\text{S}$ section. Stoichiometric amounts of elemental components corresponding to 1 g of samples were sealed under the vacuum (10^{-2} Pa) in quartz ampoules and heated up to 1000 K and kept at this temperature. After the 3 h synthesis process, all alloys were quenched in ice water and further annealed at 600 K for 1000 h in order to reach full homogenization. The PXRD results of the synthesized alloys showed that samples containing >70 mol % $\text{Sb}_2\text{Te}_2\text{S}$ contained a small amount of Sb_2Te_3 phase, that reaching a maximum amount for $\text{Sb}_2\text{Te}_2\text{S}$. Taking it into account, these non-equilibrium

alloys were ground into powder, pressed into tablets, and additionally annealed at 600 K for 500 hours. The latter powder XRD data confirmed their single-phase nature.

The NETZSCH 404 F1 Pegasus system with 10 K/min of heating and cooling rate was used for DTA. X-ray phase analysis was performed at room temperature in the range of $2\theta = 5-75$ degrees on a Bruker D2 PHASER diffractometer with $\text{CuK}\alpha_1$ radiation. Lattice parameters were calculated using the TOPAS 4.2 program. SEM analyses were performed by Tescan Vega 3 SBH Scanning Electron Microscope. For elemental analysis of samples by the EDX method, the P/B ZAF quantification method was applied.

Results and discussion

Annealed alloys of the $\text{Sb}_2\text{Te}_2\text{S}-\text{Bi}_2\text{Te}_2\text{S}$ system with 20, 40, 60, and 80 mol. % $\text{Bi}_2\text{Te}_2\text{S}$

compositions were studied by the PXRD method.

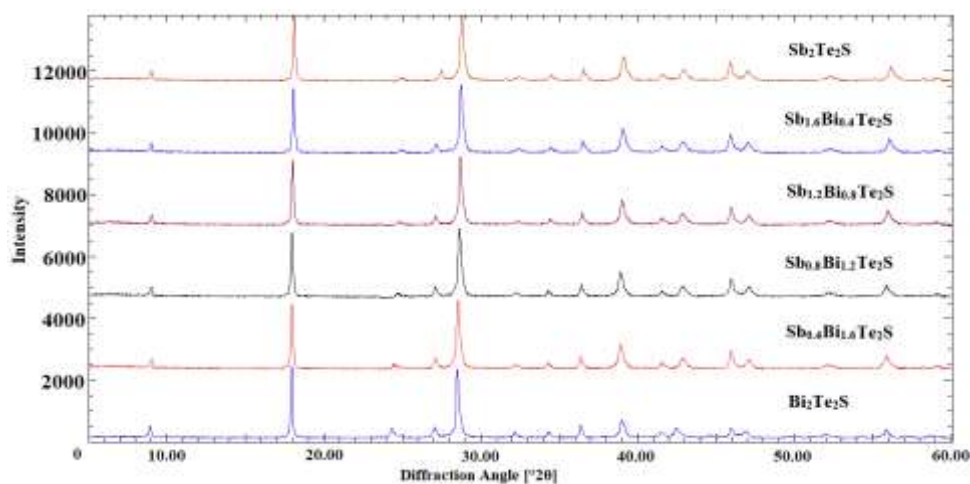


Fig.1. PXRD patterns of the alloys along the $\text{Sb}_2\text{Te}_2\text{S}-\text{Bi}_2\text{Te}_2\text{S}$ system.

Obtained X-ray diffraction patterns of the alloys are presented in Fig.1.

As can be seen, all intermediate $\text{Sb}_{2-x}\text{Bi}_x\text{Te}_2\text{S}$ alloys, as expected, are individual phases without any traces of impurities. Diffraction peaks of $\text{Sb}_2\text{Te}_2\text{S}$ are slightly shifted towards larger angles. This is due to the formation of a continuous solid solutions in this system.

Crystal lattice parameters of all alloys were determined from PXRD patterns using the

TOPAS 4.2 program (Table 1). Based on the results obtained, a graph of the dependence of lattice parameters on composition was constructed (Fig.4). As can be seen, the lattice parameters have a linear dependence on the composition, which indicates that Vegard's rule is observed.

Based on the DTA and PXRD results (Table 1, Fig. 3), the phase diagram of the $\text{Sb}_2\text{Te}_2\text{S}-\text{Bi}_2\text{Te}_2\text{S}$ system was constructed.

Table 1. DTA results and lattice parameters of the $\text{Sb}_{2-x}\text{Bi}_x\text{Te}_2\text{S}$ alloys

Composition, mol % $\text{Bi}_2\text{Te}_2\text{S}$	Thermal effects, K	Parameters of the crystal lattice, Å
$\text{Sb}_2\text{Te}_2\text{S}$	758, 853	$a = 4.1675(2)$, $c = 29.483(1)$
10	770-791-848	---
20	783-824-844	$a = 4.1877(1)$, $c = 29.503(2)$
30	798-841	---
40	812-849	$a = 4.2068(2)$, $c = 29.527(3)$
50	824-863	---
60	839-873	$a = 4.2284(1)$, $c = 29.548(2)$
70	854-878	---
80	868-883	$a = 4.2462(2)$, $c = 29.569(3)$
90	878-890	---
$\text{Bi}_2\text{Te}_2\text{S}$	893	$a = 4.2648(1)$, $c = 29.588(2)$

Figure 2 a demonstrates the DTA heating thermogram for non-homogenized as-cast $\text{Sb}_{1.6}\text{Bi}_{0.4}\text{Te}_2\text{S}$ alloy. In order to reach the equilibrium state, alloy was grounded into powder and pressed into pellet. Further, this pellet was annealed at 600 K for 500 hours.

Thermal analysis of the homogenized pellet illustrates the achievement of equilibrium state. Thermal effects at 740 K and 773 K were transformed into one peak at 783 K illustrated in the figure 2b.

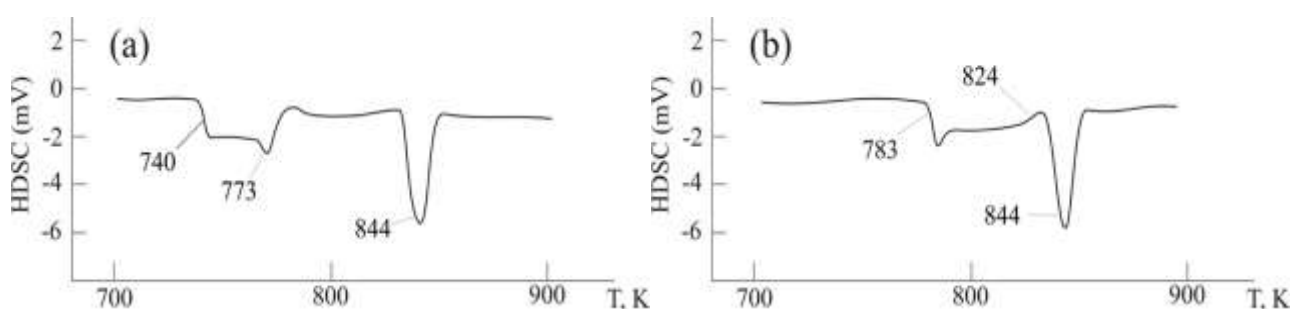


Fig. 2. DTA heating thermograms for the alloys: a) as-cast $\text{Sb}_{1.6}\text{Bi}_{0.4}\text{Te}_2\text{S}$; b) annealed $\text{Sb}_{1.6}\text{Bi}_{0.4}\text{Te}_2\text{S}$.

Figure 3 shows the phase diagram of the $\text{Sb}_2\text{Te}_2\text{S}-\text{Bi}_2\text{Te}_2\text{S}$ system. The system is partially non-quasibinary due to the incongruent melting of one of the initial compounds, $\text{Sb}_2\text{Te}_2\text{S}$. The α -phase based on Sb_2Te_3 , initially

crystallizes from the solution in the <30 mol. % $\text{Bi}_2\text{Te}_2\text{S}$ composition range. Below the liquidus of the α -phase, crystallization continues according to the monovariant peritectic reaction

$L+\alpha\leftrightarrow\gamma$, leading to the formation of an intermediate three-phase region $L+\alpha+\gamma$, which could not be detected by means of DTA. In the >30 mol. % $\text{Bi}_2\text{Te}_2\text{S}$ compositions field, crystallization proceeds according to the scheme

$L\leftrightarrow\gamma$. Excess melt crystallizes with the formation of a stable sub-solidus γ -phase and forms $\text{Bi} \leftrightarrow \text{Sb}$ cation-substituted continuous solid solutions.

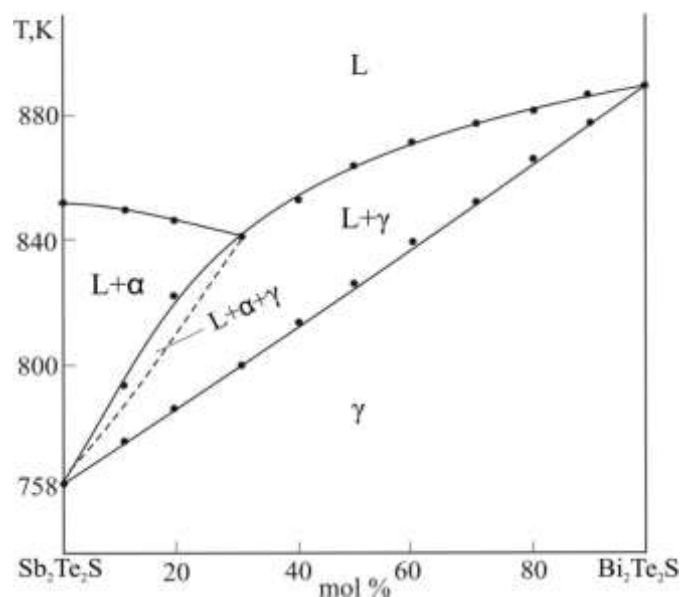


Fig. 3. The phase diagram of the $\text{Sb}_2\text{Te}_2\text{S}$ - $\text{Bi}_2\text{Te}_2\text{S}$ system

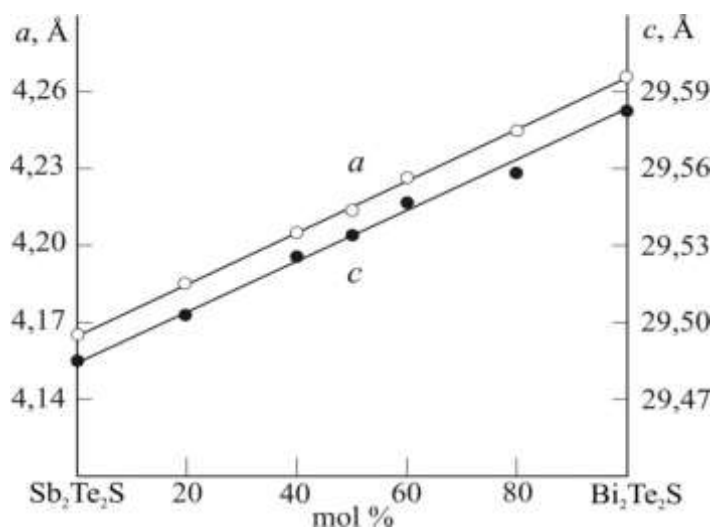


Fig. 4. Dependence of lattice parameters on composition along the $\text{Sb}_2\text{Te}_2\text{S}$ - $\text{Bi}_2\text{Te}_2\text{S}$ system

The SEM image of the sample with 40 mol. % $\text{Bi}_2\text{Te}_2\text{S}$ composition is given in the Fig.5. As can be clearly seen from the image, the sample is monophasic and has a layered structure. Results of the elemental microanalysis

by the EDX method of same sample are given in the table 2 which shows that elemental composition corresponds to the stoichiometry of the given alloy.

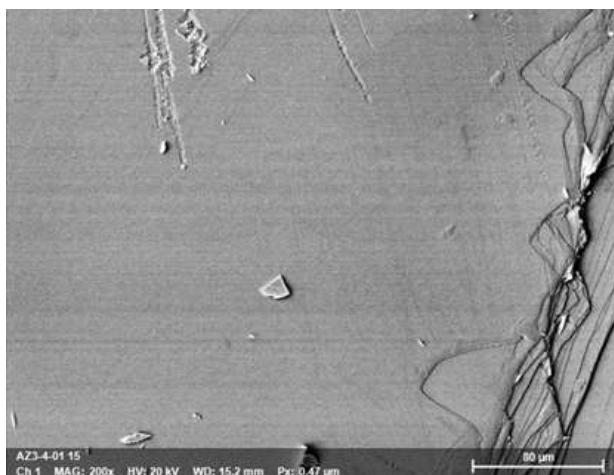


Fig.5. SEM image of the alloy containing 40% mol $\text{Bi}_2\text{Te}_2\text{S}$

Table 2. Elemental microanalysis results of the 40% mol $\text{Bi}_2\text{Te}_2\text{S}$ sample

Element	Weight %	Atom %	Error %
Antimony	23.78	22.43	0.98
Bismuth	27.45	17.37	2.78
Tellurium	41.95	43.91	1.27
Sulphur	6.82	16.29	4.10
	100	100	

Conclusion

From results of DTA, XRD, SEM and EDX investigations the phase diagram of the $\text{Sb}_2\text{Te}_2\text{S}-\text{Bi}_2\text{Te}_2\text{S}$ system was constructed. It has been established that the system is non-quasibinary as a whole, however, is stable in the subsolidus region and characterized by the formation of continuous solid solutions with a

tetradymite-like structure. Lattice parameters of solid solutions were defined to be linearly dependent upon composition. Obtained solid solutions of the $\text{Sb}_{2-x}\text{Bi}_x\text{Te}_2\text{S}$ composition have great practical interest as potential thermoelectrics and topological insulators.

References

- Maxim S., Maxim R., Yury S., Alexey S., Alexey., Egor K., Dmitry N. Thermoelectric properties of efficient thermoelectric materials on the basis of bismuth and antimony chalcogenides for multisection thermoelements. *Journal of Alloys and Compounds*. 2021, vol. 877, pp. 160328. <https://doi.org/10.1016/j.jallcom.2021.160328>
- Andzane J., Felsharuk A., Sarakovskis A., Malinovskis U., Kauranens E., Bechelany M., Niherysh K.A., Komissarov V., Erts D. Thickness-dependent properties of ultrathin bismuth and antimony chalcogenide films formed by physical vapor deposition and their application in thermoelectric generators. *Materials Today Energy*. 2021, vol. 19, pp. 100587. <https://doi.org/10.1016/j.mtener.2020.100587>
- Hegde S., Prabhu N. A review on doped/composite bismuth chalcogenide compounds for thermoelectric device applications: various synthesis techniques and challenges. *Journal of Electronic Materials*. 2022, vol. 51, no. 5, pp. 2014-2042. <https://doi.org/10.1007/s11664-022-09513-x>
- Chao H., Qiao S., Zhen L., Shi X. Thermoelectric enhancement of different kinds of metal chalcogenides. *Advanced*

- Energy Materials*. 2016, vol. 6, no. 15, pp. 1600498. <https://doi.org/10.1002/aenm.201600498>
5. Taishan Z., Ran H., Sheng G., Tian X., Prashun G., Kornelius N., Jeffrey C. Charting lattice thermal conductivity for inorganic crystals and discovering rare earth chalcogenides for thermoelectrics. *Energy Environ. Sci.*, 2021, vol. 14, no. 6, pp. 3559–3566. DOI: 10.1039/d1ee00442e
 6. Baolin X., Shihan Q., Pengbin H., Jianmin M. Antimony-and Bismuth-Based Chalcogenides for Sodium-Ion Batteries. *Chemistry—An Asian Journal*. 2019, vol. 14, no. 17, p. 2925–2937. <https://doi.org/10.1002/asia.201900784>
 7. Daniel C. Thermoelectric generators: A review of applications. *Energy Conversion and Management*. 2017, vol. 140, pp. 167–181. <https://doi.org/10.1016/j.enconman.2017.02.070>
 8. Yong C., Kang-Won J. Recent Progress in Fabrication of Antimony/Bismuth Chalcogenides for Lead-Free Solar Cell Applications. *Nanomaterials*. 2020, vol. 10, no. 11, p. 2284. <https://doi.org/10.3390/nano10112284>
 9. Priyadarshini P., Subhashree D., Ramakanta N. A review on metal-doped chalcogenide films and their effect on various optoelectronic properties for different applications. *RSC advances*. 2022, vol. 12, no. 16, pp. 9599–9620. DOI: 10.1039/D2RA00771A
 10. Seyed P., Mohammad A., Milad S., Soroush M., Fathollah P., Linge n C., Mohammad A., Ravinder K. Thermoelectric cooler and thermoelectric generator devices: A review of present and potential applications, modeling and materials. *Energy*. 2019, vol. 189, p. 115849. <https://doi.org/10.1016/j.energy.2019.07.179>
 11. Joel M. The birth of topological insulators. *Nature*. 2010, vol. 464, no. 7286, pp. 194–198. <https://doi.org/10.1038/nature08916>
 12. Zahid M., Joel M. Three-dimensional Topological Insulators. *Annual Review of Condensed Matter Physics*. 2011, vol. 2, no. 1, pp. 55–78. <https://doi.org/10.1146/annurev-conmatphys-062910-140432>
 13. Rachel S. Interacting topological insulators: a review. *Reports on Progress in Physics*. 2018, vol. 81, no. 11, p. 116501. DOI 10.1088/1361-6633/aad6a6
 14. Babanly M.B., Chulkov E.V., Aliev Z.S., Shevel'kov A.V., Amiraslanov I.R. Phase diagrams in materials science of topological insulators based on metal chalcogenides. *Russ. J. Inorg. Chem.* 2017, vol. 62, pp. 1703–1729. <https://doi.org/10.1134/S0036023617130034>
 15. Rabia S., Ganesh G., Patnaik S., Awana V. Crystal growth and characterization of bulk Sb₂Te₃ topological insulator. *Materials Research Express*. 2018, vol. 5, no. 4, pp. 046107. DOI 10.1088/2053-1591/aabc33
 16. Marco, C., Mirko P., Simone L., Lama K., Di Santo G., Evangelos P., Aliyev Z. S., Babaly M. B., Jun F., Ivana V., Aitor M., Marino M. Manipulating the topological interface by molecular adsorbates: Adsorption of Co-Phthalocyanine on Bi₂Se₃. *Nano Letters*. 2016, vol. 16, no. 6, pp. 3409–3414. <https://doi.org/10.1021/acs.nanolett.5b02635>
 17. Lamuta, C., D. Campi., A. Cupolillo., Z. S. Aliev., Babanly M. B., Chulkov E. V., Politano A., Pagnotta L. Mechanical properties of Bi₂Te₃ topological insulator investigated by density functional theory and nanoindentation. *Scripta Materialia*. 2016, vol. 121, pp. 50–55. <https://doi.org/10.1016/j.scriptamat.2016.04.036>
 18. Orujlu E. N., Ziya S. A., Mahammad B. B. The phase diagram of the MnTe–SnTe–Sb₂Te₃ ternary system and synthesis of the iso- and aliovalent cation-substituted solid solutions. *Calphad*. 2022, vol. 76, pp. 102398. <https://doi.org/10.1016/j.calphad.2022.102398>
 19. Tian W., Yu W., Shi J., Wang Y. The property, preparation and application of topological insulators: a review. *Materials*. 2017, vol. 10, no. 7, pp. 814. <https://doi.org/10.3390/ma10070814>
 20. Ming Y., Hongxi Z., Jun W. Topological insulators photodetectors: Preparation, advances and application challenges.

- Materials Today Communications*. 2022, vol. 33, pp. 104190. <https://doi.org/10.1016/j.mtcomm.2022.104190>
21. Nechaev I., Aguilera I., De Renzi V., Di Bona A., Lodi A., Mio A. M., Nicotra G., Politano A., Scalese S., Aliev Z.S., Babanly M.B., Friedrich C., Blügel S., Chulkov E.V. Quasiparticle spectrum and plasmonic excitations in the topological insulator Sb_2Te_3 . *Phys. Rev.* 2015. vol. 91, no. 24, pp. 245123. <https://doi.org/10.1103/PhysRevB.91.245123>
 22. Viti L., Coquillat D., Politano A., Kokh K.A., Aliyev Z.S., Babanly M.B., Tereshchenko O.E., Knap W., Chulkov E.V., Vitiello M.S. Plasma-Wave Terahertz Detection Mediated by Topological Insulators Surface States. *Nano Lett.* 2016. vol.16, no. 1, pp. 80–87. <https://doi.org/10.1021/acs.nanolett.5b02901>
 23. Hari P. Michael N. Three-dimensional topological insulator quantum dot for optically controlled quantum memory and quantum computing. *Physical Review B*. 2013, vol. 88, no. 8, pp. 085306. <https://doi.org/10.1103/PhysRevB.88.085316>
 24. He M., Huimin S., Qing H. Topological insulator: Spintronics and quantum computations. *Frontiers of Physics*. 2019, vol. 464, no. 7286, pp. 1-16. <https://doi.org/10.1007/s11467-019-0893-4>
 25. Grauer C., Hor S., Williams J., Cava J. Thermoelectric properties of the tetradymite-type $\text{Bi}_2\text{Te}_2\text{S-Sb}_2\text{Te}_2\text{S}$ solid solution. *Materials Research Bulletin*. 2009, vol. 44, no. 9, pp. 1926-1929. <https://doi.org/10.1016/j.materresbull.2009.05.002>
 26. Aliyev F., Babanly D. Phasa relations in the $\text{Sb}_2\text{Te}_3\text{-Sb}_2\text{S}_3$ system. *6th Internatianol Turkic World Conference on chemical sciences and technologies*. 2022, pp. 71.
 27. Elvin A., Elnur O., Dunya B., Duniyali M., Elvin A., Irada M., Nadir A., Nazim M., Mahammad B. Phase equilibria of the $\text{Sb}_2\text{Te}_3+2\text{BiI}_3\leftrightarrow\text{Bi}_2\text{Te}_3+2\text{SbI}_3$ reciprocal system: Synthesis and characterization of the cation-substituted $\text{Bi}_{1-x}\text{Sb}_x\text{TeI}$ solid solutions. *Journal of Alloys and Compounds*. 2022, vol. 929, pp. 167388. <https://doi.org/10.1016/j.jallcom.2022.167388>
 28. Shelimova E., Konstantinov P., Kretova M., Avilov E., Zemskov V. Thermoelectric properties of cation-substituted solid solutions based on layered tetradymite-like compounds. *Inorganic materials*. 2004, vol. 40, pp. 461-467. <https://doi.org/10.1023/B:INMA.0000027591.50936.18>
 29. Seidzade A., Babanly M. Phase diagram of the $\text{SnSb}_2\text{Te}_4\text{-SnBi}_2\text{Te}_4$ system and some properties of the $\text{SnSb}_{2-x}\text{Bi}_x\text{Te}_4$ solid solutions. *Azerbaijan Chemical Journal*. 2019, vol. 4, pp. 6-10. doi.org/10.32737/0005-2531-2019-4-6-10
 30. Gurbanov G., Adygezalova M. Character of Interaction in the $\text{SnSb}_2\text{Te}_4\text{-SnBi}_2\text{Te}_4$ System and the Thermoelectric Properties of $(\text{SnSb}_2\text{Te}_4)_{1-x}(\text{SnBi}_2\text{Te}_4)_x$ Solid Solutions. *Semiconductors*. 2021, vol. 55, no. 12, pp. 943-947. <https://doi.org/10.1134/S1063782621060063>
 31. Mammadli P.R., Gasimov V.A., Babanly D.M. Phase relations in the $\text{Cu}_3\text{SbS}_4\text{-Sb}_2\text{S}_3\text{-S}$ system. *Chemical Problems*. 2022, no 1(20), pp. 40-48. <https://doi.org/10.32737/2221-8688-2022-1-40-47>
 32. Babanly D.M., Tagiyev D.B. Physicochemical aspects of ternary and complex phases development based on thallium chalcogenides. *Chemical Problems*. 2018, vol. 16, no. 2, pp.153-177. DOI:[10.32737/2221-8688-2018-2-153-177](https://doi.org/10.32737/2221-8688-2018-2-153-177)

ФАЗОВЫЕ РАВНОВЕСИЯ В СИСТЕМЕ $Sb_2Te_2S-Bi_2Te_2S$ И ХАРАКТЕРИСТИКА
ТВЕРДЫХ РАСТВОРОВ $Sb_{2-x}Bi_xTe_2S$

¹Ф.Р. Алиев, ¹Э.Н. Оруджлу, ^{1,2}Д.М. Бабанлы, ³А.Л. Мустафаева

¹*Азербайджанский университет нефти и промышленности,
Французско-азербайджанский университет
Пр. Азадлыг, 20, Баку, AZ 1010*

²*Институт катализа и неорганической химии
Пр. Г.Джавида, 113, Баку, AZ 1143*

³*Бакинский государственный университет
Ул. З.Халилова, 23, Баку, AZ 1148,
e-mail: fariz_ar@hotmail.com*

Аннотация: Фазовые равновесия в системе $Sb_2Te_2S-Bi_2Te_2S$ были исследованы методами рентгенфазового анализа, дифференциального термического анализа, сканирующего электронного микроскопа и энергодисперсионного рентгеновского микроанализа. Показано, что из-за инконгруэнтного плавления соединения Sb_2Te_2S система в целом неквазибинарна, но устойчива ниже солидуса и характеризуется образованием непрерывного ряда твердых растворов с тетрадимитоподобной гексагональной структурой. По результатам порошковых дифрактограмм были определены параметры решетки. Установлено, что параметры кристаллической решетки твердых растворов линейно зависят от состава.

Ключевые слова: фазовая диаграмма, твердые растворы, тетрадимитоподобная структура, топологические изоляторы.

$Sb_2Te_2S-Bi_2Te_2S$ SİSTEMİNDƏ FAZA TARAZLIQLARI VƏ $Sb_{2-x}Bi_xTe_2S$ BƏRK
MƏHLULLARININ XASSƏLƏRİ

¹F.R. Əliyev, ¹E.N. Oruclu, ^{1,2}D.M.Babanlı, ³A.L. Mustafayeva

¹*Azərbaycan Dövlət Neft və Sənaye Universiteti, Azərbaycan-Fransız Universiteti
AZ 1010, Bakı, Azadlıq pr., 20*

²*Kataliz və Qeyri-üzvi Kimya İnstitutu
AZ 1143, Bakı, H.Cavid pr., 113*

³*Bakı Dövlət Universiteti
AZ 1148 Bakı, Z.Xəlilov küç., 23
e-mail: fariz_ar@hotmail.com*

Xülasə: $Sb_2Te_2S-Bi_2Te_2S$ sisteminin faza tarazlıqları toz rentgenfaza analizi, differensial termiki analiz, skanəedici elektron mikroskopiyası və enerji-dispersiv rentgen mikroanalizi ilə tədqiq edilmişdir. Göstərilmişdir ki, Sb_2Te_2S birləşməsinin inkonqruent əriməsi səbəbindən sistem bütövlükdə qeyri-kvazibinar olsa da solidusdan aşağıda stabildir və tetradimitəbənzər heksoqonal quruluşa malik fasiləsiz bərk məhlulların əmələ gəlməsi ilə xarakterizə olunur. Toz difraktoqramları əsasında nümunələrin qəfəs parametrləri təyin olunmuş və müəyyən edilmişdir ki, bərk məhlulların kristal qəfəs parametrləri tərkibdən asılılığı xəttidir.

Açar sözlər: faza diaqramı, bərk məhlullar, tetradimitəbənzər quruluş, topoloji izolyatorlar.